International Journal of Heat and Fluid Flow 49 (2014) 108–115

Contents lists available at ScienceDirect

International Journal of Heat and Fluid Flow

journal homepage: www.elsevier.com/locate/ijhff

Large-eddy simulation of a pseudo-shock system in a Laval nozzle

J.F. Quaatz *, M. Giglmaier, S. Hickel, N.A. Adams

Institute of Aerodynamics and Fluid Mechanics, Technische Universität München, Boltzmannstraße 15, 85748 Garching b. München, Germany

ARTICLE INFO

Article history:
Available online 10 June 2014

Keywords:
Pseudo-shock system
Nozzle flow
Large-eddy simulation
Shock-wave–boundary-layer interaction

ABSTRACT

Well-resolved Large-Eddy Simulations (LES) of a pseudo-shock system in the divergent part of a Laval nozzle with rectangular cross section are conducted and compared with experimental results. The LES matches the parameter set of a reference experiment. Details of the experiment, such as planar side walls, are taken into account, all wall boundary layers are well-resolved and no wall model is used. The Adaptive Local Deconvolution Method (ALDM) with shock sensor is employed for subgrid-scale turbulence modeling and shock capturing. The LES results are validated against experimental wall-pressure measurements and schlieren pictures. A detailed discussion of the complex flow phenomena of three-dimensional shock-wave–boundary-layer interaction, including corner vortices and recirculation zones, is presented. Limitations of RANS approaches are discussed with reference to the LES results.

1. Introduction

Depending on the applied back pressure, choked Laval nozzle flows develop a compression shock that decelerates the flow from supersonic to subsonic speed. Inviscid theory predicts an instantaneous change of the flow variables through a single normal shock. Taking viscous effects into consideration, a so-called pseudo-shock system develops at sufficiently high pre-shock Mach numbers, which is generally a sequence of several oblique shocks and expansion waves interacting with the boundary layers at the nozzle walls and a subsequent mixing zone.

Pseudo-shock systems affect the performance and the reliability of processes and facilities in many fields of engineering, see Matsuo et al. (1999) for a comprehensive overview. Although there are several previous experimental (e.g., Carroll and Dutton, 1990; Johnson and Papamoschou, 2010) and numerical (e.g., Xiao et al., 2007) studies, the mechanisms that govern the dynamic behavior of pseudo-shock systems are not yet sufficiently understood. Key mechanisms, such as the interaction between three-dimensional shocks and recirculation zones, are too complex to be analyzed and explained by experiments alone. For this flow configuration, previous numerical simulations solving the compressible Reynolds-averaged Navier–Stokes (RANS) equations show a high sensitivity of the results to details of the applied turbulence model (see Giglmaier et al., 2014). In particular, two-equation models based on the Boussinesq hypothesis give poor predictions of secondary flow features and are not able to represent the anisotropy of turbulence. Results for Reynolds stress models that are based on the ω-formulation generally are in much better agreement with experimental data. However, RANS simulations cannot recover highly unsteady small-scale phenomena. This motivates a numerical investigation with well-resolved Large-Eddy Simulation (LES).

The paper is arranged as follows: Section 2 gives an overview of the investigated experiment and describes the numerical setup of the LES. The results are validated against the measurements in Section 3. Finally, the LES is compared to RANS simulations with several standard turbulence models applied in Section 4.

2. Experiment and numerical setup

Geometry of the flow channel as well as operating conditions of this numerical investigation are adapted to a comprehensive experimental study conducted by Gawehn et al. (2010). The test rig is designed as double choked Laval nozzle system (refer to Fig. 1). The pseudo-shock system is located in the divergent part of the primary nozzle. In contrast to (quasi) constant-area ducts (e.g., Carroll and Dutton, 1990; Morgan et al., 2014), in this experiment the mean shock position is well defined by the wall contour and the applied back pressure. Parallel side walls at the primary nozzle allow for schlieren imaging. The test rig is equipped with 47 pressure taps to record the wall pressure distribution. Assuming inviscid adiabatic flow, shock position and pre-shock Mach number are defined by the ratio of the stagnation pressures p_{02}/p_{01} at the exit and the entry of the primary nozzle, which is a function of the ratio of the critical cross section areas A_1^*/A_2^*. In the experiment, the secondary critical cross section area A_2^* can be adjusted by a movable, slender cone to allow for different stagnation pressure ratios.

* Corresponding author. Tel.: +49 8928916393.
E-mail address: quaatz@tum.de (J.F. Quaatz).

http://dx.doi.org/10.1016/j.ijheatfluidflow.2014.05.006
0142-727X/

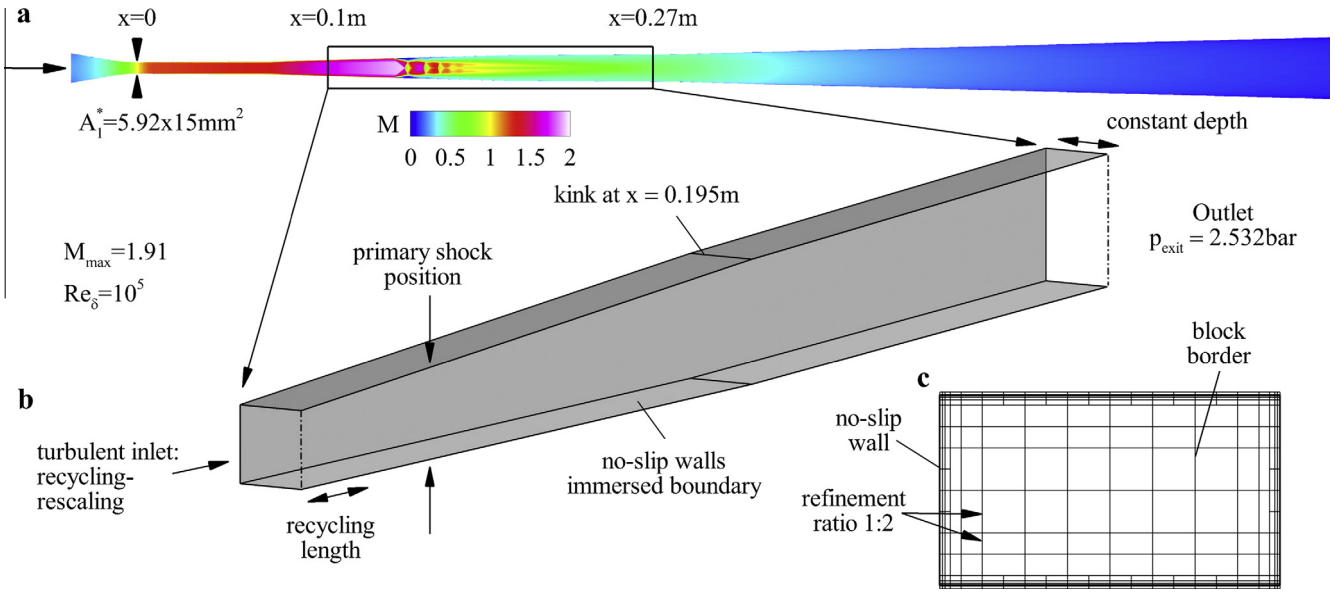

Fig. 1. Overview of the LES setup. (a) Mach number distribution at the symmetry plane $z = 0$ within the primary Laval nozzle predicted by a RANS simulation with the BSL EARSM turbulence model applied. The secondary Laval nozzle is not shown. The black box indicates the LES sub-domain. (b) Geometry and boundary conditions of the LES. Only one half is shown. (c) Sketch of the AMR block topology for the LES inlet plane.

The investigated operation point is characterized by a stagnation pressure of $p_{01} = 4.8$ bar and a stagnation temperature of $T_{01} = 300$ K. The operating fluid is air. The stagnation pressure ratio is set to $p_{02}/p_{01} = 0.6$, which results in the shock position $x_s \approx 0.135$ m measured from the primary critical cross section A_1^*. These conditions correspond to a pre-shock Mach number of $M \approx 1.91$ and a Reynolds number of $Re_\delta \approx 10^5$ based on the boundary layer thickness δ, which extends to approx. 36% of the channel half height. We emphasize, that all presented LES and RANS simulations are performed at the same parameter set – including the Reynolds number – of this reference experiment. A sketch of the apparatus and the flow conditions is given in Fig. 1a, which shows the Mach number distribution at the symmetry slice $z = 0$.

Our computer code INCA is applied for conducting the LES. The hyperbolic fluxes are discretized by the Adaptive Local Deconvolution Method ALDM (Hickel et al., 2006; Hickel and Larsson, 2009). Built into this non-linear finite-volume discretization method is a subgrid-scale turbulence model that is consistent with turbulence theory. Due to a shock sensor that triggers additional numerical viscosity over shocks, ALDM can capture shock waves while smooth pressure waves and turbulence are propagated without excessive numerical dissipation. These features make ALDM applicable to the full Mach number range of practical applications and particularly suitable for LES of shock-turbulence interactions as demonstrated, e.g., by Grilli et al. (2012, 2013). Viscous and heat conduction terms are discretized by second-order centered differences, and an explicit 3rd order Runge–Kutta method is used for time integration.

Unlike earlier work (e.g., Olson and Lele, 2011), we simulate the full 3-D geometry of the rectangular nozzle duct including both parallel side walls. Hence, effects of secondary flow features, such as geometrically induced corner vortices and flow separation, are taken into account, which is crucial for achieving agreement with experiments. To facilitate such a large-scale simulation, the computational domain is restricted to the pseudo-shock system ($0.1\text{ m} \leqslant x \leq 0.27$ m). The LES sub-domain is indicated by the black rectangle in Fig. 1a. The inflow boundary condition is located approx. 25 boundary layer thicknesses δ upstream of the primary shock. The diverging upper and lower walls consist each of two sections with the respective opening semi angles $\alpha_1 = 1.5^\circ$ and $\alpha_2 = 0.3^\circ$. The two sections are connected at $x = 0.195$ m.

INCA solves the compressible Navier–Stokes equations on Cartesian multi-block grids. It also provides a built-in mesh generator enabling adaptive mesh refinement (AMR) for efficiently resolving the channel walls. The boundary layer refinement of the block topology normal to the mean flow direction x is illustrated in Fig. 1c. The applied refinement ratio at block boundaries is set to 2. Different mesh resolutions allow for the generation of high-quality initial conditions through grid-sequencing, which strongly reduces the computational effort necessary for reaching statistically stationary flow conditions. The presented results are obtained on a grid of 387×10^6 cells in 16484 blocks. While refined grids are used for resolving turbulent boundary layers, we do not specifically refine grids at shocks in the core flow.

For representing the diverging upper and lower nozzle walls, we employ an immersed boundary method (for details see Meyer et al., 2010; Grilli et al., 2009) as shown in Fig. 1b. The parallel side walls at $z = \pm 7.5 \times 10^{-3}$ m are represented by standard no-slip conditions at the regular cell faces. Performance is improved by a linear stretching of the cells normal to the side walls. Boundary layer turbulence is resolved by the computational grid, and no wall model is applied. The non-dimensional wall-normal size of the wall cells is characterized by $\Delta y^+ \approx 2$. All walls are assumed to be adiabatic, which is reasonable for steady-state flow conditions at ambient stagnation temperature.

For generating physical turbulent inflow conditions, we use a recycling-rescaling method (Petrache et al., 2011). Mean target values for the LES inflow data at the inlet ($x_i = 0.1$ m) are extracted from a steady-state RANS simulation. It is performed with the commercial solver ANSYS CFX Release 14.0 and an explicit algebraic Reynolds stress model (EARSM – for details see Wallin and Johanson, 2000) in BSL formulation by Hellsten (2004). Giglmaier et al. (2014) give a rationale for choosing this particular RANS turbulence model. To suppress spurious periodic correlations, the recycled turbulence is additionally mirrored at the center point of the test rig, $y = z = 0$. More specifically, the fluctuations occurring in the upper right half of the channel are re-introduced into the lower left part and vice versa. The recycling length (see Fig. 1b) corresponds to approximately nine times the incoming boundary layer thickness.

A static pressure of $p_{exit} = 2.532$ bar is prescribed at the end of the LES domain. This value is taken from RANS simulations and